

# 1 **MosaicBase: A Knowledgebase of Postzygotic Mosaic Variants in**

## 2 **Noncancer Diseases and Asymptomatic Human Individuals**

3 Xiaoxu Yang<sup>1,#.a</sup>, Changhong Yang<sup>2,3,4,#.b</sup>, Xianing Zheng<sup>4,#.c</sup>, Luoxing Xiong<sup>5,d</sup>, Yutian Tao<sup>4,6,e</sup>,  
4 Meng Wang<sup>1,f</sup>, Adam Yongxin Ye<sup>1,5,g</sup>, Qixi Wu<sup>7,h</sup>, Yanmei Dou<sup>1,i</sup>, Junyu Luo<sup>4,j</sup>, Liping Wei<sup>1,\*k</sup>,  
5 August Yue Huang<sup>1,\*l</sup>

6

7 <sup>1</sup>Center for Bioinformatics, State Key Laboratory of Protein and Plant Gene Research, School of  
8 Life Sciences, Peking University, Beijing 100871, China

9 <sup>2</sup>Department of Bioinformatics, Chongqing Medical University, Chongqing, China

10 <sup>3</sup>College of Life Sciences, Beijing Normal University, Beijing 100875, China

11 <sup>4</sup>National Institute of Biological Sciences, Beijing 102206, China

12 <sup>5</sup>Peking-Tsinghua Center for Life Sciences (CLS), Academy for Advanced Interdisciplinary  
13 Studies, Peking University, Beijing 100871, China

14 <sup>6</sup>Chinese Academy of Medical Sciences and Peking Union Medical College, Beijing 100730,  
15 China

16 <sup>7</sup>School of Life Sciences, Peking University, Beijing 100871, China

17 # Xiaoxu Yang, Changhong Yang, and Xianing Zheng contributed equally to this work

18 \*Email: [weilp@mail.cbi.pku.edu.cn](mailto:weilp@mail.cbi.pku.edu.cn) (Wei L) and [huangy@mail.cbi.pku.edu.cn](mailto:huangy@mail.cbi.pku.edu.cn) (Huang A Y)

### 19 **Running title:**

20 *Yang X et al / Knowledgebase for Mosaic Variants*

21

22 <sup>a</sup>ORCID: 0000-0003-0219-0023 ([yangxx@mail.cbi.pku.edu.cn](mailto:yangxx@mail.cbi.pku.edu.cn))

23 <sup>b</sup>ORCID: 0000-0002-7573-3765 ([yangchanghong@mail.cbi.pku.edu.cn](mailto:yangchanghong@mail.cbi.pku.edu.cn))

24 <sup>c</sup>ORCID: 0000-0002-3302-1241 ([xianingz@umich.edu](mailto:xianingz@umich.edu))

25 <sup>d</sup>ORCID: 0000-0002-8884-0594 ([xiongluoxing@gmail.com](mailto:xiongluoxing@gmail.com))

26 <sup>e</sup>ORCID: 0000-0002-0360-0771 ([taoyutian@nibs.ac.cn](mailto:taoyutian@nibs.ac.cn))

27 <sup>f</sup>ORCID: 0000-0002-1072-7073 ([wangm@mail.cbi.pku.edu.cn](mailto:wangm@mail.cbi.pku.edu.cn))

28 <sup>g</sup>ORCID: 0000-0002-1542-0740 ([yeyx@mail.cbi.pku.edu.cn](mailto:yeyx@mail.cbi.pku.edu.cn))

29 <sup>h</sup>ORCID: 0000-0002-9959-2629 ([wuqixi@mail.cbi.pku.edu.cn](mailto:wuqixi@mail.cbi.pku.edu.cn))

30 <sup>i</sup>ORCID: 0000-0002-9328-1731 (douym@mail.cbi.pku.edu.cn)

31 <sup>j</sup>ORCID: 0000-0002-4679-004X (junyuluo@mednet.ucla.edu)

32 <sup>k</sup>ORCID: 0000-0002-1795-8755 (weilp@mail.cbi.pku.edu.cn)

33 <sup>l</sup>ORCID: 0000-0002-0416-2854 (huangy@mail.cbi.pku.edu.cn)

34

35 Total word counts: 2726

36 Total figures: 4

37 Total tables: 0

38 Total supplementary figures: 0

39 Total supplementary tables: 5

40 Total supplementary files: 1

41

42 **Abstract**

43 Mosaic variants resulting from postzygotic mutations are prevalent in the human genome and play  
44 important roles in human diseases. However, except for cancer-related variant collections, there  
45 are no collections of mosaic variants in noncancer diseases and asymptomatic individuals. Here,  
46 we present MosaicBase (<http://mosaicbase.cbi.pku.edu.cn/> or <http://49.4.21.8:8000/>), a  
47 comprehensive database that includes 6,698 mosaic variants related to 269 noncancer diseases and  
48 27,991 mosaic variants identified in 422 asymptomatic individuals. The genomic and phenotypic  
49 information for each variant was manually extracted and curated from 383 publications.  
50 MosaicBase supports the query of variants with Online Mendelian Inheritance in Man (OMIM)  
51 entries, genomic coordinates, gene symbols, or Entrez IDs. We also provide an integrated genome  
52 browser for users to easily access mosaic variants and their related annotations within any  
53 genomic region. By analyzing the variants collected in MosaicBase, we found that mosaic variants  
54 that directly contribute to disease phenotype showed features distinct from those of variants in  
55 individuals with a mild or no phenotype in terms of their genomic distribution, mutation  
56 signatures, and fraction of mutant cells. MosaicBase will not only assist clinicians in genetic  
57 counseling and diagnosis but also provide a useful resource to understand the genomic baseline of  
58 postzygotic mutations in the general human population.

59

60 **KEYWORDS**

61 Postzygotic, Mosaicism, Noncancer, Mutation, MosaicBase

62

63

## 64 Introduction

65 Genomic mosaicism results from postzygotic mutations arising during embryonic development,  
66 tissue self-renewal [1], aging processes [2], or exposure to other DNA-damaging circumstances  
67 [3]. Unlike *de novo* or inherited germline variants that affect every cell in the carrier individual [4],  
68 postzygotic mosaic variants only affect a portion of cells or cell populations, and their mutant  
69 allelic fractions (MAFs) should be 50% [5]. If a postzygotic mutation affects germ cells [6], the  
70 mutant allele may theoretically be transmitted to offspring, which is the major source of genetic  
71 variations in the human population [7].

72 Postzygotic mosaic variants have previously been demonstrated to be directly responsible for  
73 the etiology of cancer [8, 9] and an increasing number of other Mendelian or complex diseases,  
74 including epilepsy-related neurodevelopment disorders [10], Costello syndrome [11], autism  
75 spectrum disorders [12, 13], and intellectual disability [14]. On the other hand, pathogenic genetic  
76 variants inherited from detectable parental mosaicism have been demonstrated to be an important  
77 source of monogenic genetic disorders, including Noonan syndrome [15], Marfan syndrome [16],  
78 Dravet syndrome [17], and complex disorders, including autism [18] and intellectual disability  
79 [19]. The MAF of a mosaic variant has been reported to be directly related to the carrier's  
80 phenotype [20, 21] and to be associated with the recurrence risk in children [5].

81 With the rapid advances in next-generation sequencing (NGS) technologies, tens of  
82 thousands of postzygotic mosaic single-nucleotide variants (SNVs) and insertions/deletions  
83 (indels) have been identified and validated in the genomes of human individuals [3, 22, 23].  
84 However, except for cancer-related variants that have been collected by databases such as the  
85 Catalogue of Somatic Mutations in Cancer (COSMIC) [24] and SomamiR (somatic mutations  
86 impacting microRNA function in cancer) [25], there is no integrated database focusing on mosaic  
87 variants in noncancer diseases and asymptomatic individuals.

88 Here, we present MosaicBase (<http://mosaicbase.cbi.pku.edu.cn/> or <http://49.4.21.8:8000/>); to  
89 our knowledge, MosaicBase is the first knowledgebase of mosaic SNVs and indels identified in  
90 patients with noncancer diseases and their parents as well as asymptomatic individuals.  
91 MosaicBase currently contains 34,689 validated mosaic variants that have been manually curated  
92 from 383 publications. MosaicBase has further integrated comprehensive genomic and phenotypic

93 information about each variant and its carrier. It provides multi-scale information about  
94 disease-related mosaic variants for genetic counseling and molecular diagnosis as well as the  
95 genomic background of mosaic variants in general populations.

96

## 97 **Database implementation**

### 98 **The framework of MosaicBase**

99 An overview of the framework of MosaicBase is shown in Figure 1. MosaicBase consists of two  
100 logical parts: the database and server as the backend and the user interface as the frontend.  
101 Structured data based on three relational tables were established in the backend of MosaicBase.  
102 The storage and maintenance of the database were implemented with SQLite v3. The frontend of  
103 MosaicBase provides a user-friendly interface written in PHP, JavaScript, HTML and CSS, with  
104 Django applications.

105 MosaicBase incorporates two different search modes to help the user browse the database.  
106 The information for each mosaic variant has been summarized from the publication and individual  
107 levels to the gene and variant levels. A built-in genome browser is provided to visualize variants. A  
108 statistical summary and detailed tutorials for MosaicBase are available on the main page.  
109 MosaicBase further provides an online submission system to encourage the community to  
110 contribute to the database.

111

### 112 **Data collection, processing, and annotation**

113 We queried against the PubMed database using keywords including “mosaic”, “mosaicism”,  
114 “post-zygotic”, “somatic”, “sequencing” (see the full query string in Supplemental Text), and  
115 excluded publications about cancer-related mosaic mutations or studies on non-human organisms  
116 by examining the titles and abstracts. For more than 1,000 search results, we scrutinized the main  
117 text as well as supplemental information to confirm the relevance of each publication. After this  
118 process, 383 journal research articles about mosaic SNVs and indels in noncancer individuals that  
119 were published between Jan 1989 and May 2018 were collected into MosaicBase. For each article,  
120 data fields for the publication, individual, and variation information were extracted and saved into  
121 three tables in the backend (Figure 1). For studies involving single-cell technologies, only the

122 validated or high-confidence postzygotic mosaic SNVs were collected. For the table of variation  
123 information, we further integrated the genomic annotations generated by ANNOVAR [26],  
124 including population allele frequency from dbSNP (version 137) [27] and gnomAD (genome;  
125 version 2.0.1) [28], risk scores such as CADD scores (version 1.30) [29] and Eigen scores [30],  
126 functional predictions by FATHMM [31], SIFT [32], iFish2 [33], DeFine [34], conservation  
127 prediction by GERP++ [35] and PhyloP [36], and annotations in COSMIC [37]. A detailed  
128 description of different fields and data types required in each field is listed in Supp. Tables S1, S2,  
129 and S3. The transcript-based variation information was confirmed using Mutalyzer following the  
130 suggestions from the Human Genome Variation Society (HGVS) [38]. Genomic coordinates were  
131 provided according to the human reference genome UCSC hg19/GRCh37 as well as  
132 hg38/GRCh38.

133 **Statistical analysis and visualization of mosaic variants**

134 The mutation signature analysis has been widely used in cancer studies to elaborate the etiology of  
135 somatic mosaic variants, by decomposing the matrix of tri-nucleotide context into cancer-related  
136 signatures. In this study, the signature of noncancer mosaic variants was analyzed by Mutalisk  
137 [39], and the maximum likelihood estimation of proportions for each mutation signature was  
138 performed based on a greedy algorithm. For each variant group, we further tested whether its  
139 genomic density within each 1 Mb interval was correlated with the GC content, DNase I  
140 hypersensitive regions, replication timing, and histone modification profiles measured in the  
141 GM12878 cell line [39]. A genome browser based on the Dalliance platform [40] was  
142 implemented to interactively visualize the mosaic variants. Circos [41] was utilized to show the  
143 genomic distribution of mosaic variants.

144

145 **Web interface**

146 **User interface and functions**

147 We incorporated two search modes in MosaicBase. The basic search mode provided on the main  
148 page recognizes search terms based on the name of diseases, the range of genomic coordinates,  
149 gene symbols, or Entrez Gene IDs (Figure 2A), in which the search engine is comparable with  
150 space-delimited multiple search terms. The result page of the basic search mode displays variant

151 summary information according to the categories of search terms, and search results can then be  
152 downloaded as an xls format table. We also introduced an ontology-based search mode as an  
153 advanced option in MosaicBase; with this mode, users can browse the mosaic variants related to a  
154 specific disease or disease category according to the Disease Ontology [42]. A brief summary of  
155 the description of the disease or disease category is provided along with a summary table of all the  
156 related mosaic variants collected in MosaicBase (Figure 2B).

157 Detailed information about each mosaic variant was summarized in four different panels in  
158 MosaicBase: the overview panel, the gene information panel, the individual information panel,  
159 and the publication information panel (Figure 2C). In the overview panel, we provided the  
160 genomic information as well as the methodologies for the identification and validation of the  
161 variant. In the gene information panel, we annotated the Entrez Gene ID, official gene symbol and  
162 alternative names, number of reported mosaic variants in this gene, Vega ID, OMIM ID, HGNC  
163 ID, Ensembl ID, and a brief summary of the gene. In the gene information panel, we summarized  
164 all the collected mosaic variants in the same gene and provided various resources for gene  
165 annotation from external databases, including Entrez, Vega, OMIM, HGNC, and Ensembl IDs. In  
166 the individual information panel, we classified the phenotypes of the individual carrying the  
167 mosaic variant and displayed the information according to the original descriptions in the  
168 publication. The severity of phenotype collected in MosaicBase was defined as “1” if the carrier  
169 was asymptomatic, “2” if the carrier had a mild phenotype but did not fulfill all the diagnostic  
170 criteria for a specific disease or characterized syndrome, and “3” if the carrier fulfilled all the  
171 clinical diagnostic criteria for a specific disease. In the publication information panel, we  
172 summarized the title, journal, sample, and additional information about the publication that  
173 reported the mosaic variant.

174 MosaicBase integrated a build-in genome browser to provide convenient interactive data  
175 visualization for the mosaic variants (Figure 2D). In addition to the default tracks about genetic  
176 and epigenetic annotations, such as DNase I hypersensitive sites and H3K4me predictions,  
177 MosaicBase also allows the user to import customized tracks from URLs, UCSC-style track hubs,  
178 or uploaded files in a UCSC-style genome browser track format. The URLs for tracks of Ensembl  
179 Gene and MeDIP-seq data are provided as examples, and a help page providing detailed guidance  
180 is also available by clicking the question mark in the top-left panel of the genome browser.

181 MosaicBase further provided users with an application that can generate publication-quality SVG  
182 files from the control panel of the genome browser.

183 MosaicBase included a “Statistics” page to show a summary of all the collected mosaic  
184 variants (Figure 2E) and a “Tutorials” page (Figure 2F) with detailed introductions about the  
185 database and its search modes, data presentation, and genome browser. We also implemented an  
186 online submission system that allows users to submit mosaic variants from newly published or  
187 uncollected publications. Such variants will be manually examined by our team and integrated into  
188 MosaicBase with scheduled updates.

189

#### 190 **Statistical analysis of noncancer mosaic variants**

191 MosaicBase currently includes 383 journal research articles, letters, and clinical genetic reports  
192 about noncancer postzygotic mosaic variants that were published from 1989 to 2018 (Figure 3A),  
193 with an accelerated accumulation of mosaic-related publications boosted by the recent advances in  
194 NGS technologies. After manually extracting the mosaic variants reported in each publication, we  
195 thoroughly compiled 34,689 mosaic variants from 2,202 noncancer individuals, including 6,698  
196 disease-related variants from 3,638 genes related to 269 noncancer diseases as well as 27,991  
197 apparently neutral variants identified from 442 asymptomatic individuals (Figure 3B and Supp.  
198 Table S4). Specifically, two types of disease-related mosaic variants were collected in MosaicBase:  
199 1) 6,207 mosaic variants that had directly contributed to the disease phenotype in 1,402 patients  
200 (323 men and 197 women; 882 sex unknown from the original publication) and 2) 491 mosaic  
201 variants identified from 358 parents or grandparents (137 men and 193 women; 28 sex unknown  
202 from the original publication) of the probands who had transmitted the mosaic allele to their  
203 offspring for a heterozygous genotype that led to disease phenotypes (Figure 3B). The collected  
204 mosaic variants were classified into three groups according to the origin of the variants described  
205 in the original publications: variants from asymptomatic individuals were termed the “asym”  
206 group; variants from patients fulfilling the full diagnostic criteria of a specific disease were termed  
207 the “patient” group; variants from parents/grandparents of the patients were termed the “parent”  
208 group. As shown in Figure 3C, mosaic variants were generally distributed across all the autosomes  
209 and X chromosomes. Parental mosaic variants were clustered in the *SCN1A* gene on chromosome  
210 2, which resulted from the well-studied parental mosaic cases for Dravet syndrome. The

211 underrepresentation of mosaic variants in the Y chromosome might be explained by its low gene  
212 density and the technical challenge of detecting mosaic variants in haplotype chromosomes.

213 To study whether mosaic variants from different groups of individuals have distinct genomic  
214 characteristics, we calculated their correlation with various genomic regulation features, including  
215 GC content, DNase I hypersensitive positions, and epigenetic modifications. Because the vast  
216 majority of mosaic variants had been identified from peripheral blood or saliva samples, genomic  
217 regulation patterns of GM12878, a lymphoblastoid-derived cell line, were used in the subsequent  
218 analysis. Common germline variants annotated in dbSNP 137 with allele frequency higher than  
219 10% (“dbSNP” group) were served as a control. According to the Pearson correlation coefficients  
220 between the signal intensities of genomic features and the density of variants with a window size  
221 of 1MB across the genome [43], we found that the mosaic variants that directly contribute to the  
222 disease phenotype (“patient” group) are more positively correlated with such genomic features  
223 than the mosaic variants of the other groups (Figure 4A).

224 Next, we examined the mutation spectrum of the mosaic variants. Similar to inherited  
225 germline variants [44] and somatic mutations reported in cancer studies [45], C>T is the most  
226 predominant type for mosaic variants (Figure 4B). We then extracted the tri-nucleotide genomic  
227 context of each variant and decomposed the matrix into mutation signatures previously identified  
228 in various types of cancers (<https://cancer.sanger.ac.uk/cosmic/signatures>). Single base mutation  
229 signature analysis further revealed that over 50% of the mosaic variants can be decomposed into  
230 the combination of cancer signatures 1, 5 and 30 (Figure 4C). Signatures 1 and 5 result from the  
231 age-related process of spontaneous or enzymatic deamination of 5-methylcytosine to thymine;  
232 signatures 18 and 30 result from deficient base excision repair [46]; signature 2 indicated the  
233 activation of AID/APOBEC cytidine deaminase; signatures 6 and 20 are associated with defective  
234 DNA mismatch repair; signature 22 is associated with aristolochic acid exposure; the etiology of  
235 signatures 8, 12, 19, 25 are unknown, and signatures 51 and 58 are potential sequencing artefacts.  
236 Detailed descriptions of the signatures are provided in Supplemental Text.

237 To explore the general relationship between the MAF of a mosaic variant and the carrier  
238 phenotype, we extracted the allele fraction and phenotypic severity information for each mosaic  
239 variant in MosaicBase. For mosaic variants in the “parent” group, we observed that the mosaic  
240 variants in parents with milder or full disease phenotypes had significantly higher MAFs than

241 those of asymptomatic parents ( $P = 5.9 \times 10^{-5}$  by a two-tailed Mann-Whitney U test with continuity  
242 correction, Figure 4D), which is in accordance with previous estimations [18, 20, 47]. When we  
243 considered mosaic variants in all the collected individuals, the difference became even more  
244 significant ( $P < 2.2 \times 10^{-16}$  by a two-tailed Mann-Whitney U test, Figure 4D). These results  
245 highlighted the importance of the MAF information of mosaic variants in clinical applications  
246 such as genetic counseling.

247

## 248 **Discussion**

249 MosaicBase currently contains 34,689 mosaic SNVs and indels identified in patients with  
250 noncancer diseases and their parents, as well as asymptomatic individuals, with rich information at  
251 the publication, individual, gene and variant levels. The user-friendly interface of MosaicBase  
252 allows users to access our database by multiple searching methods and the integrated genome  
253 browser.

254 The pathogenic contribution of mosaic variants to noncancer diseases has been increasingly  
255 recognized in the past few years. MosaicBase provides genetic and phenotypic information about  
256 6,698 disease-related mosaic variants in 269 noncancer diseases. This database may help  
257 clinicians understand the pathogenesis and inheritance of mosaic variants and shed new light on  
258 future clinical applications, such as genetic counseling and diagnosis. On the other hand, the  
259 collection of 27,991 mosaic variants that were identified in asymptomatic individuals could be  
260 useful for understanding the genomic baseline of postzygotic mutations in the general human  
261 population. MosaicBase also integrates risk prediction from multiple computational tools for each  
262 variants. Unlike germline variants which are present in all cells of the carriers, mosaic variants are  
263 only present in a fraction of cells, in which the level of mosaic fraction can be an additional factor  
264 contributing to variant pathogenicity [18, 20]. In the future, with the increasing number of  
265 mosaic-related studies, we would expect a well-benchmarked scoring system specifically designed  
266 for predicting the deleterious probability of mosaic variants.

267 Of the 34689 mosaic variants collected in MosaicBase, only 0.7% to 8.7% were present in  
268 large-scale population polymorphism databases (Supp. Table 5). If we only considered common  
269 SNPs with population allele frequency (AF) higher than 0.01, the overlapping proportion further

270 reduced to 0.1% to 0.7%. This suggested that MosaicBase provided a unique set of human genetic  
271 variants which had been overlooked in previous genomic studies. Indeed, these apparently benign  
272 variants which are generated *de novo* show characteristics distinct from those of the variants that  
273 directly contribute to a disease phenotype, and also different from polymorphisms that are fixed in  
274 population under selective pressure (Figure 4). The data from MosaicBase will also encourage  
275 researchers to reanalyze existing NGS data of human diseases by mosaic variant calling tools,  
276 such as MosaicHunter [48], Mutect2 [49], and Strelka [50], to identify previously ignored disease  
277 causative variants.

278 In the future, our team will update MosaicBase regularly by collecting and reviewing new  
279 publications in PubMed and publications submitted through our online submission system. After  
280 each update, we will update the statistics and release update reports on the website. We plan to  
281 further improve the user interface of MosaicBase and add new analysis tools based on feedback  
282 from the community.

283

## 284 **Authors' contributions**

285 AYH, LW, and XY, conceived the idea of building the database about mosaic variants, XZ, XY,  
286 and CY designed and implemented the website. XY, CY, LX, YT, YD, QW, and JL collected the  
287 data. MW, and AYY assisted in the website development. XY and XZ analyzed the data from the  
288 website. XY, CY, XZ, and AYH wrote the manuscript. AYH and LW led the project.

289

## 290 **Competing interests**

291 The authors declare no competing interests.

292

## 293 **Acknowledgments**

294 This work was supported by the National Natural Science Foundation of China (No. 31530092)  
295 and the Ministry of Science and Technology of China (2015AA020108). We thank Dr. Lei Kong,  
296 Dr. Ge Gao, and Mr. Dechang Yang from the Centre for Bioinformatics, Peking University, for  
297 their efforts in helping to set up the hardware environments and maintaining the MosaicBase  
298 server. We thank Drs. Sijin Cheng and Jinpu Jin for their suggestions for the database.

## 299 References

300 [1] Huang AY, Yang X, Wang S, Zheng X, Wu Q, Ye AY, et al. Distinctive types of postzygotic  
301 single-nucleotide mosaisms in healthy individuals revealed by genome-wide profiling of multiple  
302 organs. *PLoS Genet* 2018;14:e1007395.

303 [2] Holstege H, Pfeiffer W, Sie D, Hulsman M, Nicholas TJ, Lee CC, et al. Somatic mutations found in  
304 the healthy blood compartment of a 115-yr-old woman demonstrate oligoclonal hematopoiesis.  
305 *Genome Res* 2014;24:733-42.

306 [3] Martincorena I, Roshan A, Gerstung M, Ellis P, Van Loo P, McLaren S, et al. Tumor evolution.  
307 High burden and pervasive positive selection of somatic mutations in normal human skin. *Science*  
308 2015;348:880-6.

309 [4] Freed D, Stevens EL, Pevsner J. Somatic mosaicism in the human genome. *Genes (Basel)*  
310 2014;5:1064-94.

311 [5] Ye AY, Dou Y, Yang X, Wang S, Huang AY, Wei L. A model for postzygotic mosaisms quantifies  
312 the allele fraction drift, mutation rate, and contribution to de novo mutations. *Genome Res* 2018.

313 [6] Biesecker LG, Spinner NB. A genomic view of mosaicism and human disease. *Nat Rev Genet*  
314 2013;14:307-20.

315 [7] Poduri A, Evrony GD, Cai X, Walsh CA. Somatic mutation, genomic variation, and neurological  
316 disease. *Science* 2013;341:1237758.

317 [8] Lawrence MS, Stojanov P, Mermel CH, Robinson JT, Garraway LA, Golub TR, et al. Discovery  
318 and saturation analysis of cancer genes across 21 tumour types. *Nature* 2014;505:495-501.

319 [9] Mari F, Azimonti S, Bertani I, Bolognese F, Colombo E, Caselli R, et al. CDKL5 belongs to the  
320 same molecular pathway of MeCP2 and it is responsible for the early-onset seizure variant of Rett  
321 syndrome. *Hum Mol Genet* 2005;14:1935-46.

322 [10] Stosser MB, Lindy AS, Butler E, Retterer K, Piccirillo-Stosser CM, Richard G, et al. High  
323 frequency of mosaic pathogenic variants in genes causing epilepsy-related neurodevelopmental  
324 disorders. *Genet Med* 2017.

325 [11] Gripp KW, Stabley DL, Nicholson L, Hoffman JD, Sol-Church K. Somatic mosaicism for an  
326 HRAS mutation causes Costello syndrome. *Am J Med Genet A* 2006;140:2163-9.

327 [12] Freed D, Pevsner J. The Contribution of Mosaic Variants to Autism Spectrum Disorder. *PLoS  
328 Genet* 2016;12:e1006245.

329 [13] Krupp DR, Barnard RA, Duffourd Y, Evans SA, Mulqueen RM, Bernier R, et al. Exonic Mosaic  
330 Mutations Contribute Risk for Autism Spectrum Disorder. *Am J Hum Genet* 2017;101:369-90.

331 [14] Gilissen C, Hehir-Kwa JY, Thung DT, van de Vorst M, van Bon BW, Willemsen MH, et al.  
332 Genome sequencing identifies major causes of severe intellectual disability. *Nature* 2014;511:344-7.

333 [15] Tartaglia M, Cordeddu V, Chang H, Shaw A, Kalidas K, Crosby A, et al. Paternal germline origin  
334 and sex-ratio distortion in transmission of PTPN11 mutations in Noonan syndrome. *Am J Hum Genet*  
335 2004;75:492-7.

336 [16] Tekin M, Cengiz FB, Ayberkin E, Kendirli T, Fitoz S, Tutar E, et al. Familial neonatal Marfan  
337 syndrome due to parental mosaicism of a missense mutation in the FBN1 gene. *Am J Med Genet A*  
338 2007;143A:875-80.

339 [17] Xu X, Yang X, Wu Q, Liu A, Yang X, Ye AY, et al. Amplicon Resequencing Identified Parental  
340 Mosaicism for Approximately 10% of "de novo" SCN1A Mutations in Children with Dravet Syndrome.  
341 *Hum Mutat* 2015;36:861-72.

342 [18] Dou Y, Yang X, Li Z, Wang S, Zhang Z, Ye AY, et al. Postzygotic single-nucleotide mosaicism  
343 contribute to the etiology of autism spectrum disorder and autistic traits and the origin of mutations.  
344 *Hum Mutat* 2017;38:1002-13.

345 [19] Acuna-Hidalgo R, Bo T, Kwint MP, van de Vorst M, Pinelli M, Veltman JA, et al. Post-zygotic  
346 Point Mutations Are an Underrecognized Source of De Novo Genomic Variation. *Am J Hum Genet*  
347 2015;97:67-74.

348 [20] Yang X, Liu A, Xu X, Yang X, Zeng Q, Ye AY, et al. Genomic mosaicism in paternal sperm and  
349 multiple parental tissues in a Dravet syndrome cohort. *Sci Rep* 2017;7:15677.

350 [21] de Lange IM, Koudijs MJ, van 't Slot R, Gunning B, Sonsma ACM, van Gemert L, et al.  
351 Mosaicism of de novo pathogenic SCN1A variants in epilepsy is a frequent phenomenon that correlates  
352 with variable phenotypes. *Epilepsia* 2018.

353 [22] Huang AY, Xu X, Ye AY, Wu Q, Yan L, Zhao B, et al. Postzygotic single-nucleotide mosaicism in  
354 whole-genome sequences of clinically unremarkable individuals. *Cell Res* 2014;24:1311-27.

355 [23] Vijg J, Dong X, Zhang L. A high-fidelity method for genomic sequencing of single somatic cells  
356 reveals a very high mutational burden. *Exp Biol Med (Maywood)* 2017;242:1318-24.

357 [24] Forbes SA, Beare D, Boutselakis H, Bamford S, Bindal N, Tate J, et al. COSMIC: somatic cancer  
358 genetics at high-resolution. *Nucleic Acids Res* 2017;45:D777-D83.

359 [25] Bhattacharya A, Ziebarth JD, Cui Y. SomamiR: a database for somatic mutations impacting  
360 microRNA function in cancer. *Nucleic Acids Res* 2013;41:D977-82.

361 [26] Wang K, Li M, Hakonarson H. ANNOVAR: functional annotation of genetic variants from  
362 high-throughput sequencing data. *Nucleic Acids Res* 2010;38:e164.

363 [27] Sherry ST, Ward MH, Kholodov M, Baker J, Phan L, Smigielski EM, et al. dbSNP: the NCBI  
364 database of genetic variation. *Nucleic Acids Res* 2001;29:308-11.

365 [28] Karczewski KJ, Francioli LC, Tiao G, Cummings BB, Alföldi J, Wang Q, et al. Variation across  
366 141,456 human exomes and genomes reveals the spectrum of loss-of-function intolerance across  
367 human protein-coding genes. *bioRxiv* 2019.

368 [29] Kircher M, Witten DM, Jain P, O'Roak BJ, Cooper GM, Shendure J. A general framework for  
369 estimating the relative pathogenicity of human genetic variants. *Nat Genet* 2014;46:310-5.

370 [30] Ionita-Laza I, McCallum K, Xu B, Buxbaum JD. A spectral approach integrating functional  
371 genomic annotations for coding and noncoding variants. *Nat Genet* 2016;48:214-20.

372 [31] Shihab HA, Gough J, Cooper DN, Stenson PD, Barker GL, Edwards KJ, et al. Predicting the  
373 functional, molecular, and phenotypic consequences of amino acid substitutions using hidden Markov  
374 models. *Hum Mutat* 2013;34:57-65.

375 [32] Ng PC, Henikoff S. SIFT: Predicting amino acid changes that affect protein function. *Nucleic  
376 Acids Res* 2003;31:3812-4.

377 [33] Wang M, Wei L. iFish: predicting the pathogenicity of human nonsynonymous variants using  
378 gene-specific/family-specific attributes and classifiers. *Sci Rep* 2016;6:31321.

379 [34] Wang M, Tai C, E W, Wei L. DeFine: deep convolutional neural networks accurately quantify  
380 intensities of transcription factor-DNA binding and facilitate evaluation of functional non-coding  
381 variants. *Nucleic Acids Res* 2018;46:e69.

382 [35] Davydov EV, Goode DL, Sirota M, Cooper GM, Sidow A, Batzoglou S. Identifying a high  
383 fraction of the human genome to be under selective constraint using GERP++. *PLoS Comput Biol*  
384 2010;6:e1001025.

385 [36] Pollard KS, Hubisz MJ, Rosenbloom KR, Siepel A. Detection of nonneutral substitution rates on

386 mammalian phylogenies. *Genome Res* 2010;20:110-21.

387 [37] Reva B, Antipin Y, Sander C. Predicting the functional impact of protein mutations: application to  
388 cancer genomics. *Nucleic Acids Res* 2011;39:e118.

389 [38] Wildeman M, van Ophuizen E, den Dunnen JT, Taschner PE. Improving sequence variant  
390 descriptions in mutation databases and literature using the Mutalyzer sequence variation nomenclature  
391 checker. *Hum Mutat* 2008;29:6-13.

392 [39] Lee J, Lee AJ, Lee JK, Park J, Kwon Y, Park S, et al. Mutualisk: a web-based somatic MUTation  
393 AnaLyIS toolKit for genomic, transcriptional and epigenomic signatures. *Nucleic Acids Res*  
394 2018;46:W102-W8.

395 [40] Down TA, Piipari M, Hubbard TJ. Dalliance: interactive genome viewing on the web.  
396 *Bioinformatics* 2011;27:889-90.

397 [41] Krzywinski M, Schein J, Birol I, Connors J, Gascoyne R, Horsman D, et al. Circos: an information  
398 aesthetic for comparative genomics. *Genome Res* 2009;19:1639-45.

399 [42] Kibbe WA, Arze C, Felix V, Mitraka E, Bolton E, Fu G, et al. Disease Ontology 2015 update: an  
400 expanded and updated database of human diseases for linking biomedical knowledge through disease  
401 data. *Nucleic Acids Res* 2015;43:D1071-8.

402 [43] Schuster-Bockler B, Lehner B. Chromatin organization is a major influence on regional mutation  
403 rates in human cancer cells. *Nature* 2012;488:504-7.

404 [44] Conrad DF, Keebler JE, DePristo MA, Lindsay SJ, Zhang Y, Casals F, et al. Variation in  
405 genome-wide mutation rates within and between human families. *Nat Genet* 2011;43:712-4.

406 [45] Alexandrov LB, Nik-Zainal S, Wedge DC, Aparicio SA, Behjati S, Biankin AV, et al. Signatures of  
407 mutational processes in human cancer. *Nature* 2013;500:415-21.

408 [46] Helleday T, Eshtad S, Nik-Zainal S. Mechanisms underlying mutational signatures in human  
409 cancers. *Nat Rev Genet* 2014;15:585-98.

410 [47] Yang X, Gao H, Zhang J, Xu X, Liu X, Wu X, et al. ATP1A3 mutations and genotype-phenotype  
411 correlation of alternating hemiplegia of childhood in Chinese patients. *PLoS One* 2014;9:e97274.

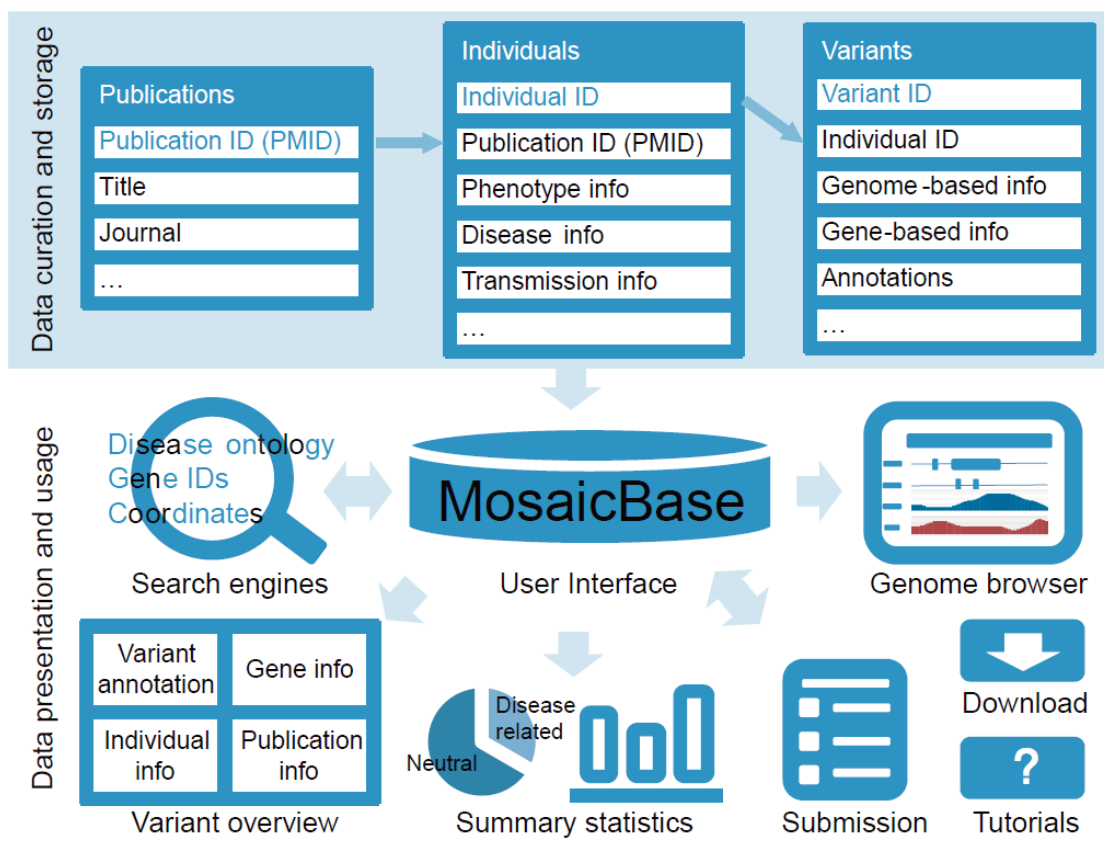
412 [48] Huang AY, Zhang Z, Ye AY, Dou Y, Yan L, Yang X, et al. MosaicHunter: accurate detection of  
413 postzygotic single-nucleotide mosaicism through next-generation sequencing of unpaired, trio, and  
414 paired samples. *Nucleic Acids Res* 2017;45:e76.

415 [49] Cibulskis K, Lawrence MS, Carter SL, Sivachenko A, Jaffe D, Sougnez C, et al. Sensitive  
416 detection of somatic point mutations in impure and heterogeneous cancer samples. *Nat Biotechnol*  
417 2013;31:213-9.

418 [50] Kim S, Scheffler K, Halpern AL, Bekritsky MA, Noh E, Kallberg M, et al. Strelka2: fast and  
419 accurate calling of germline and somatic variants. *Nat Methods* 2018;15:591-4.

420

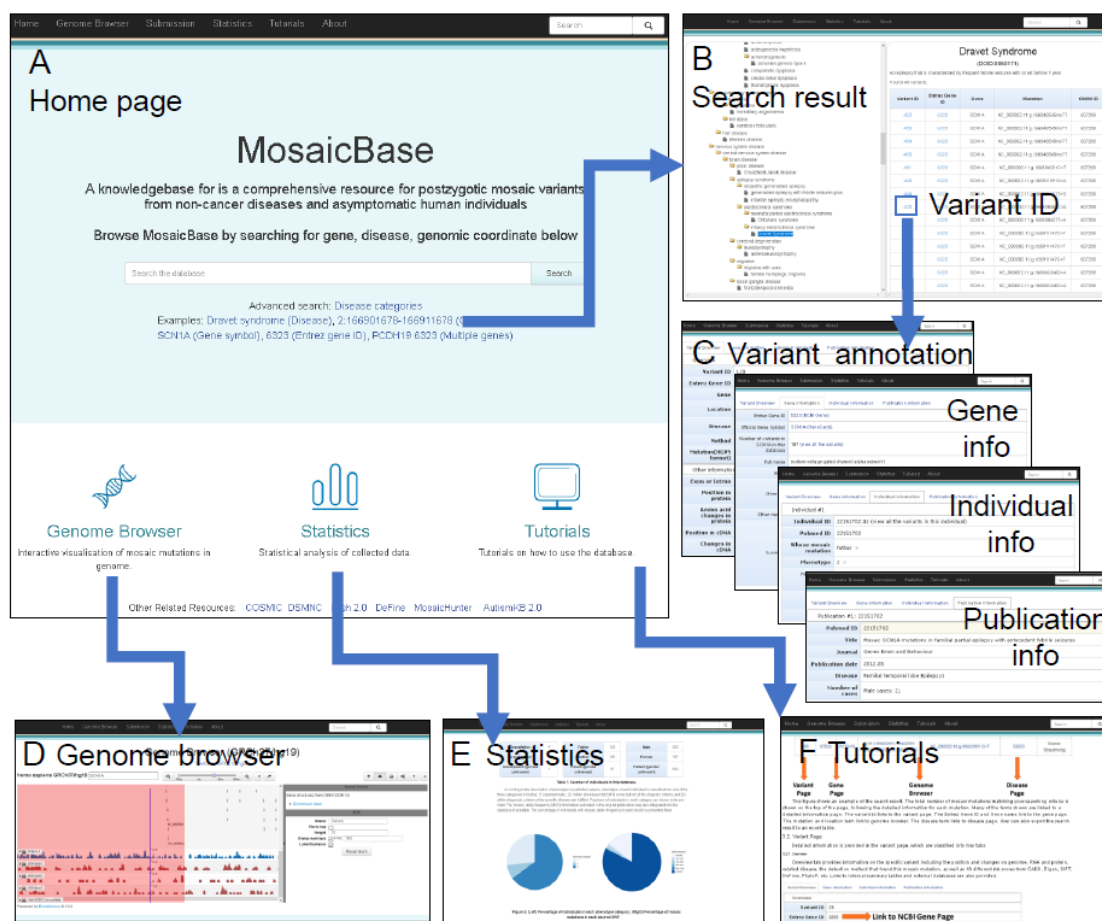
421 **Figures and Legends**



422

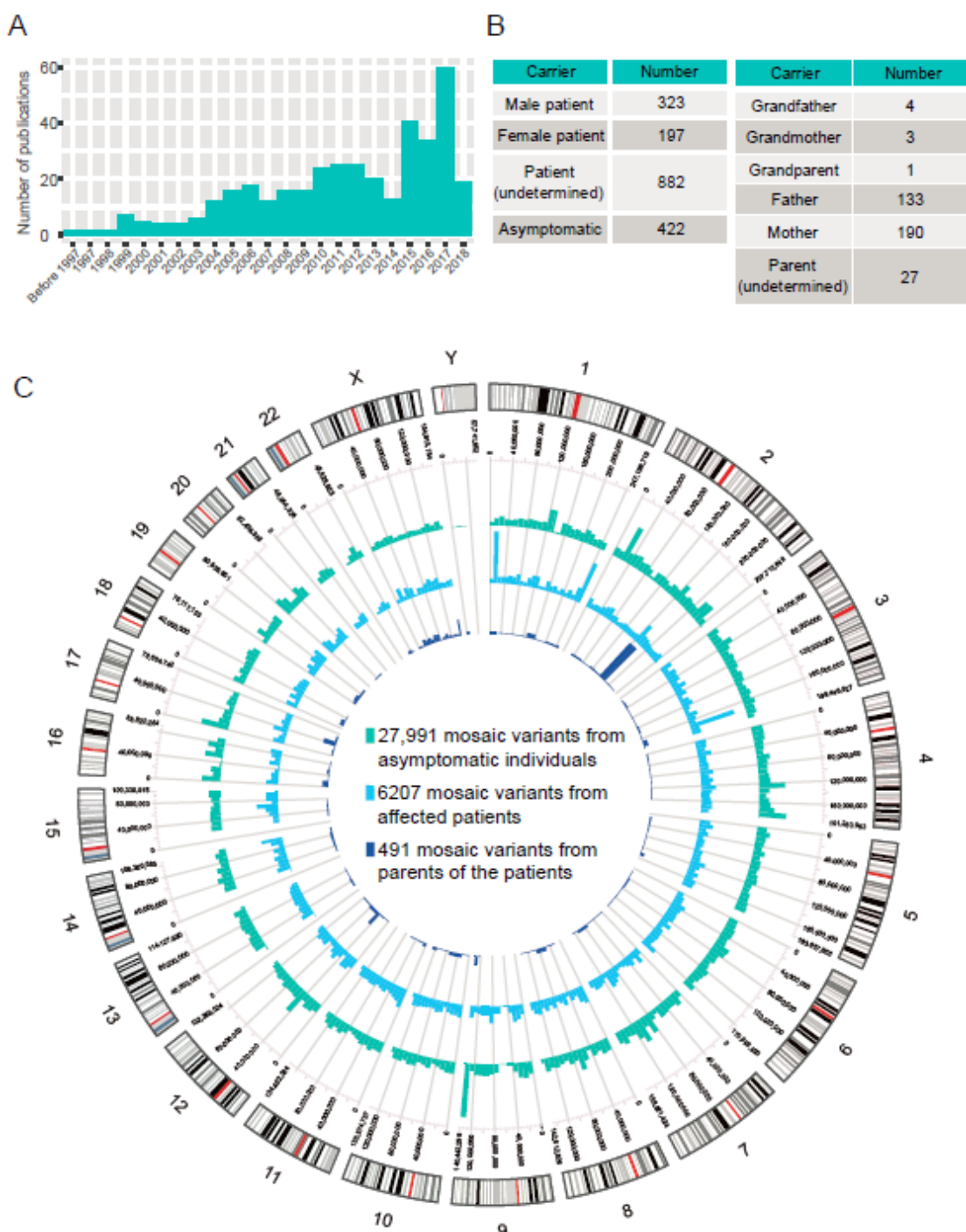
423 **Figure 1: Overview of the data collection, storage, and visualization of MosaicBase.**

424



426 **Figure 2: Screenshots of MosaicBase.**

427 A. The main page provides the search modes and multiple links to different utilities of the  
428 database. **B.** Disease-ontology-based advanced search page and an example of a result table. **C.**  
429 The variant pages from the basic search results; this page provides information about each variant  
430 and its corresponding gene, individual and publication annotation, the individuals carrying the  
431 same variant, and the publication describing the variant. **D.** Summary statistics of the publications,  
432 mutational spectrum, and individuals collected in MosaicBase. **E.** Integrated genome browser to  
433 visualize mosaic variants with genetic and epigenetic annotations. **F.** Detailed tutorials for the  
434 introduction, data presentation, and usage of MosaicBase.

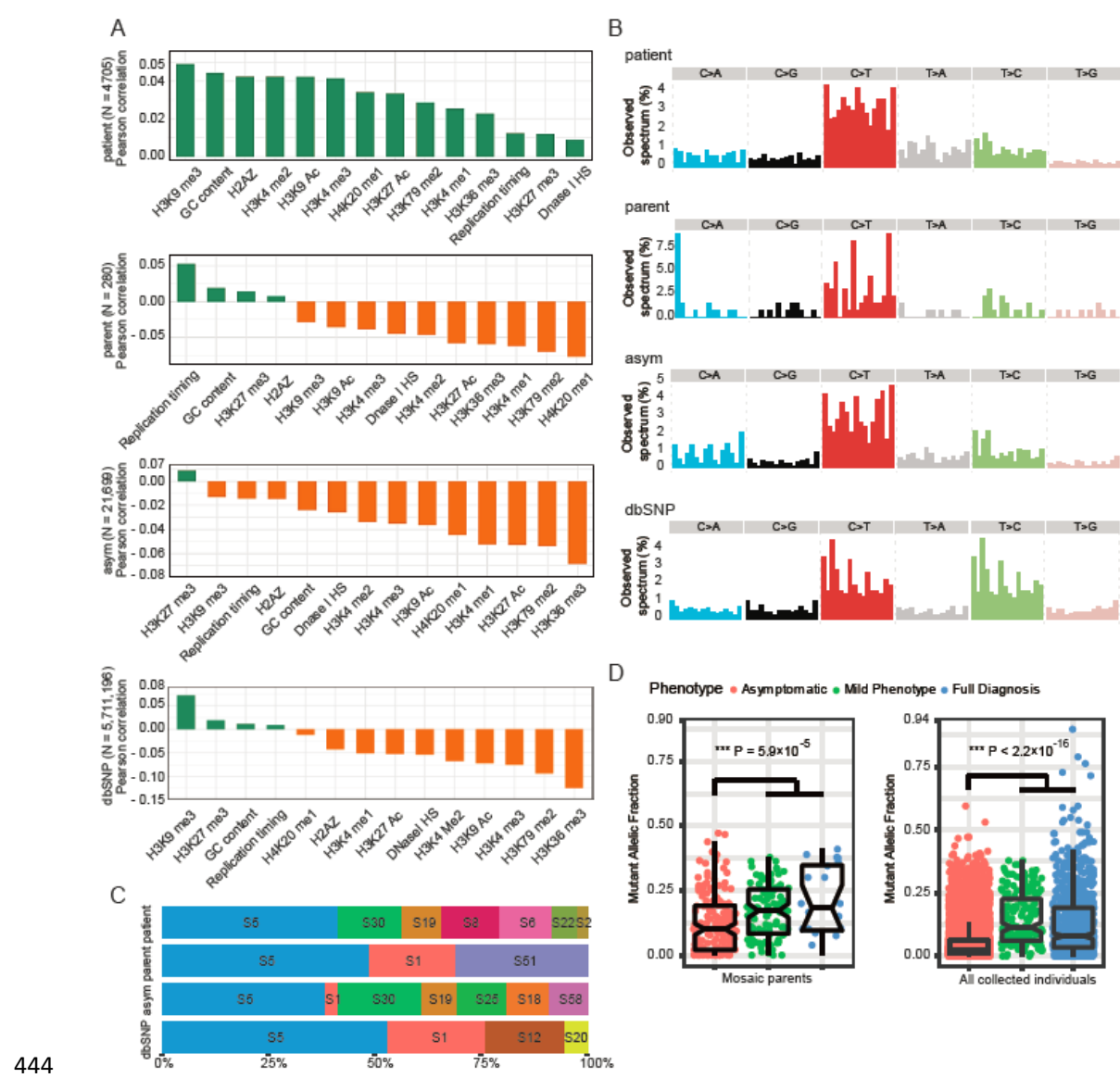


436

437 **Figure 3: Statistics about the publication, individual, and variant data collected in**  
438 **MosaicBase.**

439 A. Number of mosaic-related publications from 1989 to 2018. B. Summary of different categories  
440 of mosaic carriers. C. Circos plot of mosaic variants. Histograms show the number of mosaic  
441 variants for each 1 Mb genomic window. Chromosomal bands are illustrated in the outer circle  
442 with centromeres in red.

443



444 **Figure 4: Genomic features of mosaic variants collected in MosaicBase. A.** Correlation of the  
445 density of mosaic variants and various genomic regulation features. **B.** Tri-nucleotide genomic  
446 context of mosaic variants. **C.** Proportion of cancer signatures for mosaic variants. **D.** Mutant  
447 allele fraction of mosaic variants in mosaic parents only ( $P = 5.9 \times 10^{-5}$  by a Mann–Whitney U test  
448 with continuity correction, left) and in all individuals ( $P < 2.2 \times 10^{-16}$  by a Mann–Whitney U test,  
449 right). Common germline variants with population allele frequency  $\geq 0.1$  in dbSNP were shown  
450 for comparison.  
451

452

453 **Supplemental Materials**

454 **Supplemental Text:**

455 Literature curation and variant collection.

456 Detail description of single base substitution signatures.

457 Web Resources.

458 **Supplemental Tables:**

459 Supp. Table S1: Field description for the table of publication information.

460 Supp. Table S2: Field description for the table of individual information.

461 Supp. Table S3: Field description for the table of variation information.

462 Supp. Table S4: Summary for mosaic SNVs and indels in noncancer diseases and asymptomatic  
463 individuals in MosaicBase.

464 Supp. Table S5: Comparisons between postzygotic mosaic variants and human genetic variations  
465 identified by large-scale sequencing projects.

466 **Supplemental References**